

# **DLVO Theory and Non-DLVO Forces**

**Dr. Pallab Ghosh**  
**Associate Professor**  
**Department of Chemical Engineering**  
**IIT Guwahati, Guwahati–781039**  
**India**

**Table of Contents**

<b>Section/Subsection</b>	<b>Page No.</b>
3.5.1 DLVO theory	3
3.5.2 Non-DLVO forces	8–13
3.5.2.1 Hydration force	9
3.5.2.2 Hydrophobic interaction	11
3.5.3 Steric force due to adsorbed polymeric molecules	13
Exercise	16
Suggested reading	17

### 3.5.1 DLVO theory

- ◆ The net interaction between two surfaces involves both the electrostatic double layer force and the van der Waals force. The van der Waals force dominates when the separation between the surfaces is small. It is also rather insensitive on the concentration of the electrolytes. On the other hand, the electrostatic double layer repulsion is strong at larger separations, and it is quite sensitive on the concentration of electrolytes.
- ◆ The effects of these forces on the interaction energy are quantitatively described by the DLVO theory (named after the Russian scientists B. Derjaguin and L. Landau, and Dutch scientists E. Verwey and J. Overbeek), which was developed in the 1940s. The details of this theory have been presented by Verwey and Overbeek (1948).
- ◆ This theory has proved to be quintessential for explaining the stability of a variety of colloidal materials. It proposed that an energy barrier resulting from the repulsive force prevents two particles approaching one another and adhering together. If the particles collide with sufficient energy to overcome the barrier, the van der Waals attractive force will attract them strongly and cause them adhere together irreversibly. If the particles repel each other strongly, the dispersion will resist coagulation and the colloidal system will be stable. If the repulsion is not sufficient then coagulation will take place. The rigorous experimental verification of this theory was made in the 1970s using ‘molecularly smooth’ sheets of mica interacting in aqueous electrolyte solutions.
- ◆ Let us consider the interaction energy between two planar surfaces. The net interaction energy is the resultant of the double layer and van der Waals interaction energies. Therefore,

$$\phi_{\text{net}} = \phi_{\text{EDL}} + \phi_{\text{vdW}} = \left( 64kTn^{\infty} \kappa^{-1} \right) \tanh^2 \left( \frac{ze\psi_0}{4kT} \right) \exp(-\kappa\delta) - \frac{A_H}{12\pi\delta^2} \quad (3.5.1)$$

- ◆ Three main parameters on which the net interaction energy depends are Hamaker constant ( $A_H$ ), surface potential ( $\psi_0$ ) and concentration of electrolyte in the

bulk ( $n^\infty$ ). The Debye length,  $\kappa^{-1}$ , depends on the concentration of electrolyte [see Eq. (3.3.17)].

- ◆ Although Eq. (3.5.1) is valid for the planar surfaces, a similar development and the discussion apply to the spheres as well. The net force of interaction can be calculated from the sum of the forces due to electrostatic double layer and van der Waals force using the relation between force and interaction energy given by Eq. (3.1.9).
- ◆ The effect of variation of Hamaker constant on the energy profiles is shown in Fig. 3.5.1. The procedure to compute the Hamaker constant was discussed in Sections 3.1.9 and 3.2.2.

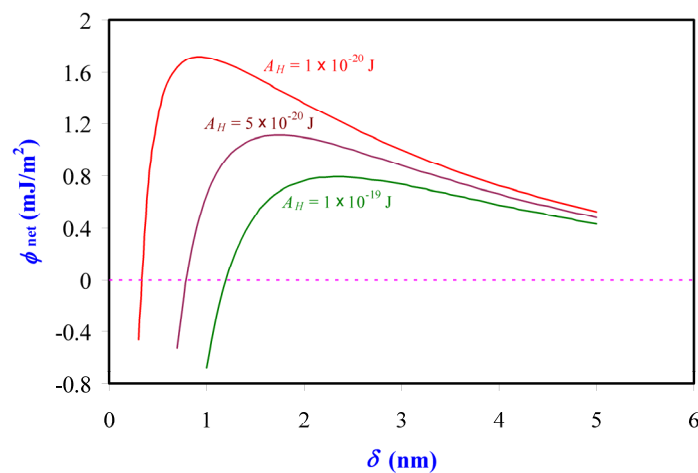


Fig. 3.5.1 Effect of Hamaker constant on DLVO profile ( $c^\infty = 10 \text{ mol/m}^3$ ,  $\kappa^{-1} = 3 \text{ nm}$  and  $\psi_0 = 100 \text{ mV}$ ).

- ◆ The profiles in Fig. 3.5.1 were drawn for the Hamaker constants of  $1 \times 10^{-20} \text{ J}$ ,  $5 \times 10^{-20} \text{ J}$  and  $1 \times 10^{-19} \text{ J}$  for surfaces placed in a  $10 \text{ mol/m}^3$  aqueous solution of a 1:1 electrolyte at 298 K. The energy barrier (i.e., the peak of the curves) decreased with the increasing value of Hamaker constant. The energy barrier shifted to larger separations with the increase in Hamaker constant.
- ◆ The effect of variation of surface potential is shown in Fig. 3.5.2.

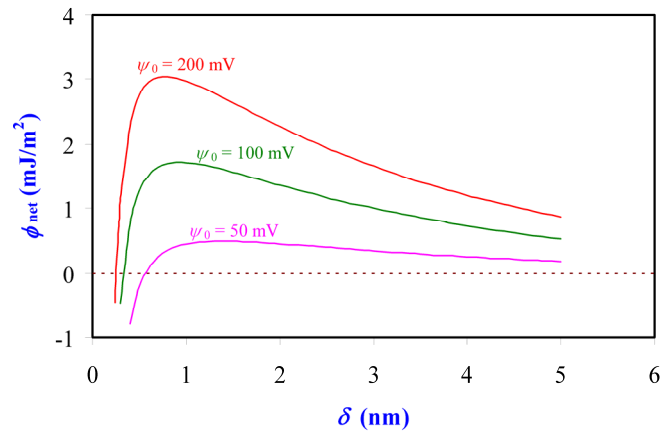


Fig. 3.5.2 The effect of variation of surface potential on the net interaction energy profiles ( $c^\infty = 10 \text{ mol/m}^3$ ,  $\kappa^{-1} = 3 \text{ nm}$ ,  $A_H = 1 \times 10^{-20} \text{ J}$ ).

- ◆ It can be observed from this figure that the energy barrier increased as the potential was increased. The term,  $\tanh^2\left(\frac{ze\psi_0}{4kT}\right)$ , in Eq. (3.5.1) approaches unity at the high values of  $\psi_0$ . Therefore, the effect of surface potential begins to reduce at the higher values. Slow coagulation of the colloid particles occurs when the energy barrier is low. At very low values of  $\psi_0$ , the energy barrier drops below  $\phi_{\text{net}} = 0$  (shown by the dotted line in the figure) and coagulation occurs rapidly.
- ◆ The effect of concentration of electrolyte on net interaction energy is depicted in Fig. 3.5.3.

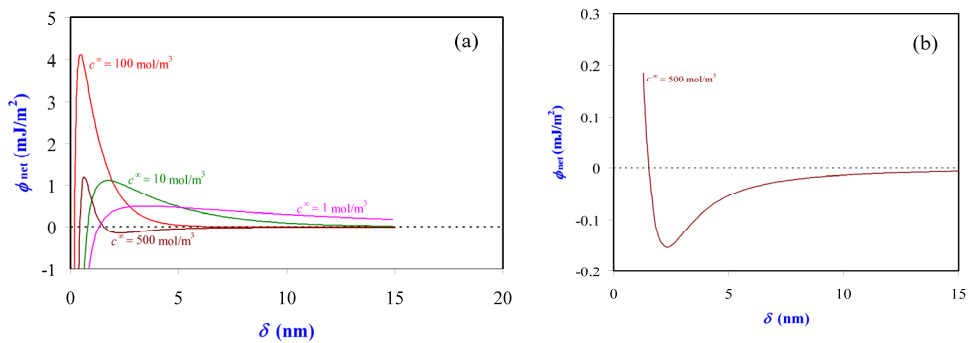


Fig. 3.5.3 (a) The effect of variation of electrolyte concentration on the net interaction energy profiles, and (b) the secondary minimum in detail ( $A_H = 5 \times 10^{-20} \text{ J}$  and  $\psi_0 = 100 \text{ mV}$ ).

- ◆ As the concentration of the electrolyte is increased,  $n^\infty$  in Eq. (3.5.1) increases but  $\kappa^{-1}$  decreases. The resulting effect is the shift in the energy barrier to a lower separation and the emergence of a *secondary minimum* [shown in the Fig. 3.5.3 (b)].
- ◆ The energy is minimum at contact, which is termed *primary minimum*. For a colloidal system, the thermodynamic equilibrium state may be reached when the particles are in deep primary minimum. However, the energy barrier may be too high so that it is difficult to overcome. In such a situation, the colloid particles may sit in the secondary minimum, which is weaker than the primary minimum. The adhesion at secondary minimum can be reversible. The secondary minimum usually appears beyond  $\delta = 2$  nm depending on the value of the Hamaker constant.
- ◆ The width of the energy barrier increases with the decreasing concentration of the electrolyte because of the increasing extension of the diffuse double layer. In the lower range of electrolyte concentration (e.g.,  $1 \text{ mol/m}^3$ – $100 \text{ mol/m}^3$ ), the height of the energy barrier increases with increase in electrolyte concentration. However, when the concentration of electrolyte is increased further (e.g.,  $500 \text{ mol/m}^3$ ), however, the energy barrier decreases. At very high electrolyte concentrations ( $> 1000 \text{ mol/m}^3$ ) attraction prevails at all values of  $\delta$ .
- ◆ The Hamaker constant is an important parameter for the energy profiles. Verwey and Overbeek (1948) have shown that the energy barrier decreases with increasing electrolyte concentration for spherical particles at all salt concentrations. This happens due to the divergence of the lines of force for the spherical particles.
- ◆ In many practical applications, the surface potential decreases with increasing electrolyte concentration (e.g., due to the binding of counterions). This helps to coagulate colloid particles at a lower concentration of the electrolyte.
- ◆ The concentration of electrolyte at which the energy barrier reduces below the  $\phi_{\text{net}} = 0$  line is known as *critical coagulation concentration*. The colloid particles

are unstable at this concentration and they coagulate rapidly (see Lecture 2 of Module 1).

**Example 3.5.1:** Calculate the net interaction energy profile for two planar surfaces at 298 K if  $\psi_0 = 100$  mV,  $A_H = 1 \times 10^{-20}$  J and  $c^\infty = 10$  mol/m<sup>3</sup> (1:1 electrolyte).

**Solution:** At  $c^\infty = 10$  mol/m<sup>3</sup> of a 1:1 electrolyte, the Debye length,  $\kappa^{-1} = 3.04$  nm and  $\kappa = 0.329$  nm<sup>-1</sup>. From Eq. (3.5.1) we have,

$$\phi_{\text{net}} = 64 \times 8.314 \times 298 \times 10 \times 3.04 \times 10^{-9} \tanh^2 \left( \frac{1.602 \times 10^{-19} \times 0.1}{4 \times 1.381 \times 10^{-23} \times 298} \right) \times \exp(-0.329\delta) - \frac{1 \times 10^{-20}}{12 \times \pi \times 10^{-18} \delta^2} \text{ J/m}^2$$

In this equation,  $\delta$  is in nanometers. The above equation, upon simplification, becomes,

$$\phi_{\text{net}} = 2.7211 \times 10^{-3} \exp(-0.329\delta) - \frac{2.6526 \times 10^{-4}}{\delta^2} \text{ J/m}^2$$

The plot of  $\phi_{\text{net}}$  versus  $\delta$  has been shown in Fig. 3.5.4.

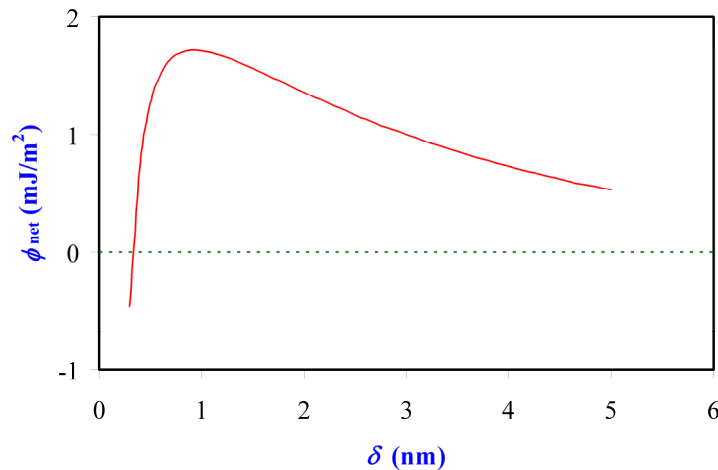


Fig. 3.5.4 Variation of net interaction energy with separation between the flat surfaces.

- ◆ Predictions from the DLVO theory have been found to be in good agreement with many experimental results on thin liquid films, swelling of clays and interaction between mica and sapphire surfaces. The force between two curved sheets of

cleaved mica in aqueous solutions of the chlorides of alkaline earth metals is shown in Fig. 3.5.5.

- ◆ The DLVO theory has been successful in explaining some of the well-known observations in colloid science such as the Schulze–Hardy rule (see Section 1.2.5). The amount of research reported in the literature to verify the validity of the DLVO theory is quite voluminous. See the texts by Israelachvili (1997), Hunter (2005), and the references cited therein to get a more detailed information on the applications of the DLVO theory.

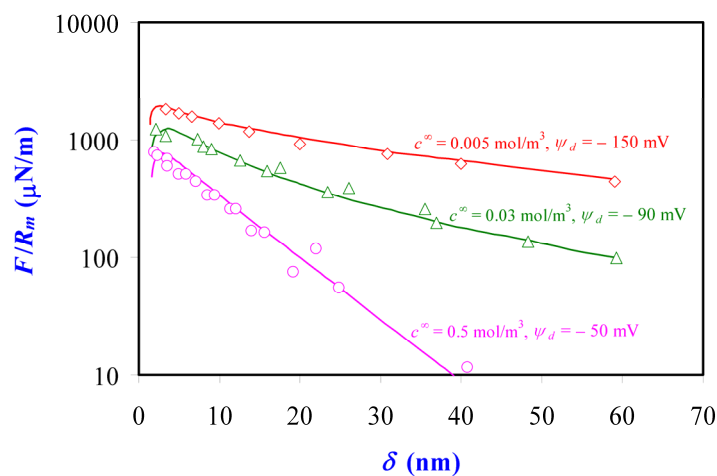


Fig. 3.5.5 The interaction force measured between two curved sheets of muscovite mica (mean radius =  $R_m$ ) in aqueous solutions of  $\text{MgCl}_2$ ,  $\text{CaCl}_2$ ,  $\text{SrCl}_2$  and  $\text{BaCl}_2$  ( $\text{pH} = 5.8 \pm 0.2$ ). The lines show the predictions from the DLVO theory ( $A_H = 2.2 \times 10^{-20}$  J) (Pashley and Israelachvili, 1984) (adapted by permission from Elsevier Ltd., © 1984).

### 3.5.2 Non-DLVO forces

- ◆ We will discuss two important forces which were not taken into account in the classical DLVO theory. Since they were not introduced in the classical DLVO theory, they are known as *non-DLVO forces*.
- ◆ These two major non-DLVO forces are *hydration force* and *hydrophobic interaction*. The former has strong effect below  $\sim 5$  nm whereas the latter force is strong when the separation between the surfaces is below  $\sim 8$  nm. These

separations can vary to some extent from one system to another and therefore, these values provide an approximate idea about the separation between the surfaces where the effects of these forces can be significant.

### 3.5.2.1 Hydration force

- ◆ The DLVO theory has successfully explained the stability and coagulation of many colloidal systems. There have been quantitative agreements between the experimental data and the DLVO theory (Claesson *et al.*, 1984; Pashley and Israelachvili, 1984).
- ◆ In many of these studies, a strong short-range repulsive force was observed at very low separations ( $< 5$  nm) at certain concentrations of the electrolyte. The repulsion was observed at separations where the van der Waals force is expected to be stronger than the double layer force. Therefore, coagulation to primary minimum is expected if the third force were absent.
- ◆ Coagulation was prevented by this short-range repulsive force. This repulsion is often due to the *hydration force*. The magnitude of the disjoining pressure due to the hydration force can be very large, of the order of 5 MPa or more, which may far exceed the electrostatic double layer repulsive pressure at that separation.
- ◆ Hydration force has proved to be very important in the stability of colloid particles, coalescence of bubbles, swelling of clays, stability of soap films and biomembrane interactions (Israelachvili and Wennerström, 1996).
- ◆ The hydration force in soap films made of cationic surfactant decyltrimethylammonium decyl sulfate in presence of sodium bromide is shown in Fig. 3.5.6.
- ◆ This stabilization is a result of the interaction between the hydration layers of very small thickness which have two flanking surfactant monolayers (Clunie *et al.*, 1967). If the film thickness is represented by  $t$ , the separation between these two layers is  $t - 2.8$  nm.

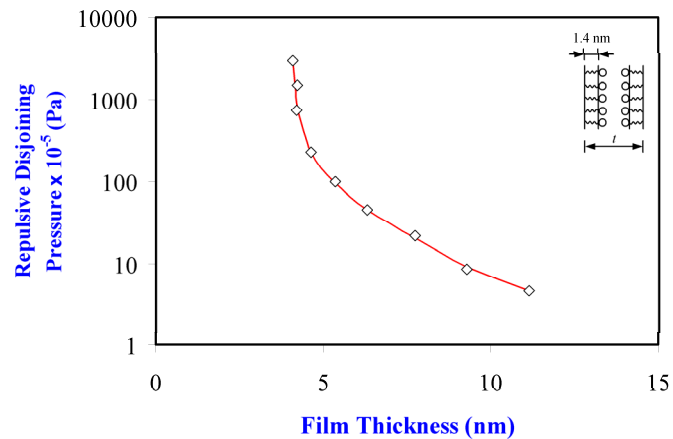


Fig. 3.5.6 *Hydration force in soap films*. The variation of repulsive pressure with film thickness for soap films made of decyltrimethylammonium decyl sulfate in presence of NaBr (Clunie et al., 1967) (adapted by permission from Macmillan Publishers Ltd., © 1967).

- ◆ For hydrophilic surfaces, the polar or ionic head-groups are hydrated. A surface which is not inherently hydrophilic can be rendered behaving like a hydrophilic surface by the adsorption of hydrated ions. This is known as *secondary hydration*.
- ◆ The hydration force arises when the adsorbed hydrated cations are prevented from desorbing as two interacting surfaces approach each other (Pashley, 1981). The adsorbed cations retain some of their water of hydration on binding. Dehydration of the adsorbed cations leads to a repulsive hydration force. The strength of the hydration force follows the order:  $\text{Mg}^{+2} > \text{Ca}^{+2} > \text{Li}^{+} \sim \text{Na}^{+} > \text{K}^{+} > \text{Cs}^{+}$ . The hydrated radius of the ions and the hydration number (i.e., the number of water molecules bound by these ions) follow similar sequences. When only protons adsorb on the surface (e.g., in acid solutions), hydration force is not observed, because the protons penetrate into the surface (Israelachvili, 1997).
- ◆ The repulsive hydration force ( $F$ ) between two hydrophilic surfaces (of radius of curvature  $R_m$ ) has been found to follow the following relation (Pashley, 1982).

$$F/R_m = C_1 \exp(-\delta/\lambda_1) + C_2 \exp(-\delta/\lambda_2) \quad (3.5.2)$$

where  $\lambda_1$  and  $\lambda_2$  are known as *decay lengths*, and  $C_1$  and  $C_2$  are constants.

- ◆ For aqueous solutions of 1:1 electrolytes such as LiCl, NaCl, KCl and CsCl, it has been found that the values of  $C_1$  lie between 0.17 and 0.25 N/m, and the values

of  $C_2$  lie between 0.014 and 0.06 N/m. For the same electrolytes, the shorter decay length,  $\lambda_1$ , varies between 0.17 and 0.3 nm, and the longer decay length,  $\lambda_2$ , varies between 0.6 and 1.1 nm. See Lecture 4 of Module 8 for further discussion on the hydration forces.

### 3.5.2.2 *Hydrophobic interaction*

- ◆ The force of attraction between hydrocarbons such as hexane, cyclohexane or benzene, is much stronger than that one would expect if the force were due to van der Waals interaction alone. The van der Waals energy of interaction for these hydrocarbons in water at room temperature is about 0.2 kJ/mol, which is much lower than the experimentally measured values, which is nearly equal to 10 kJ/mol.
- ◆ At the same time, the calculated van der Waals attraction between two water molecules or two hydrocarbon molecules is greater than the attractive force between a water molecule and a hydrocarbon molecule. This is one of the reasons why the hydrocarbons and halocarbons do not dissolve in water to any significant extent but separate out in different phases.
- ◆ These compounds are called *hydrophobic* and their water-fearing property due to which they separate out in different phases is termed *hydrophobic effect*. When a hydrocarbon molecule comes in contact with water, the surrounding water molecules can engulf it with their hydrogen bonds if the size of the hydrocarbon molecule is small. This is known as *hydrophobic hydration*. Such hydration is, however, energetically unfavorable because the free energy of the system increases by this process.
- ◆ The origin of hydrophobic interaction is a subject of debate. Since it is quite strong, some scientists believe that there is a ‘hydrophobic bond’ between the molecules. On the other hand, some scientists believe that the hydrophobic effect is essentially entropic. It generates mainly due to the configurational rearrangement of the water molecules around the hydrocarbon molecules. Hydrophobic interaction involves a further structural rearrangement of water

molecules as two solute (hydrocarbon) molecules come together. Therefore, according to this theory, the range of interaction has to be significantly larger than any bond.

- ◆ An example of hydrophobic interaction between two mica surfaces made hydrophobic by the adsorption of cationic surfactant cetyltrimethylammonium bromide is shown in Fig. 3.5.7.

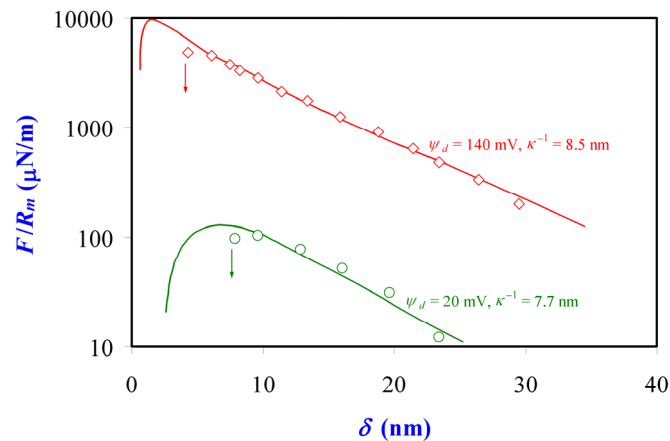


Fig. 3.5.7 The hydrophobic interaction force  $F$  measured between two curved sheets of mica (mean radius =  $R_m$ ) on which CTAB was adsorbed. For the upper curve, pH = 5.6, CTAB concentration =  $0.025 \text{ mol/m}^3$  and KBr concentration =  $1.3 \text{ mol/m}^3$ . For the lower curve, pH = 9, CTAB concentration =  $0.1 \text{ mol/m}^3$  and KBr concentration =  $1.5 \text{ mol/m}^3$ . The lines show the predictions from the DLVO theory using  $A_H = 2 \times 10^{-20} \text{ J}$ . (Israelachvili and Pashley, 1984) (adapted by permission from Elsevier Ltd., © 1984).

- ◆ It can be observed that the energy barrier predicted by the DLVO theory occurred at a much lower separation than the separation where the hydrophobic attraction caused the surfaces to come to the primary minimum (indicated by the arrows in the figure).
- ◆ The hydrophobic force varies with separation by the following exponential decay law (Israelachvili and Pashley, 1984).

$$F/R_m = -C_3 \exp(-\delta/\lambda_3) \quad (3.5.3)$$

where  $C_3$  is a constant and  $\lambda_3$  is the decay length. Hydrophobic interaction plays an important role in the fusion of lipid bilayers, which will be discussed in Lecture 4 of Module 8.

### 3.5.3 Steric force due to adsorbed polymeric molecules

- ◆ Coagulation of colloid particles can be prevented by adding polymers which are soluble in the liquid and can adsorb on the surface of these particles. Synthetic as well as biopolymers are frequently used to stabilize colloids. The adsorbed layers of the polymer on two particles repel each other. This type of repulsion between two surfaces is termed *steric repulsion*.
- ◆ However, a polymer chain may cause coagulation by *bridging*. The repulsion between surfaces covered with polymeric molecules begins when the segments of the polymer begin to overlap. The adsorbed layers encounter reduction in entropy when confined in a very small space as two surfaces approach each other. Since the reduction in entropy is thermodynamically unfavorable, their approach is inhibited.
- ◆ Let us consider the approach of two flat surfaces on which there are adsorbed or grafted chains of polymer as shown in Fig. 3.5.8.

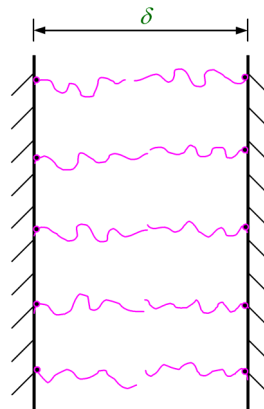


Fig. 3.5.8 Interaction between polymer layers adsorbed on flat surfaces leading to steric repulsion.

- ◆ The polymer is completely soluble in the solvent. The surfaces are well-covered by the polymer and they are brought close to each other without any bridging.

The thickness of the polymer brush,  $L$ , can be related to the number of segments of the polymer molecule,  $n_s$ , and the length of each segment,  $l$ , by the following equation (Israelachvili, 1997),

$$L = \frac{n_s l^{5/3}}{\bar{s}^{2/3}}, \quad \bar{s} = (1/\Gamma)^{1/2} \quad (3.5.4)$$

where  $\bar{s}$  is the mean distance between the attachment points and  $\Gamma$  is the number of adsorbed chains per unit area (assuming that each polymer molecule is grafted at one end to the surface).

- ◆ The polymer brushes come into contact when  $\delta = 2L$ . If the separation between the surfaces falls below  $2L$ , the concentration of polymer inside the brushes increases. This gives two contributions to the force: (i) the osmotic pressure inside each brush increases, and (b) the elastic restoring force which tends to thin out the brush decreases. The repulsive pressure developed between the surfaces can be calculated from the de Gennes equation (de Gennes, 1987),

$$\Pi_s = \frac{kT}{\bar{s}^3} \left[ \left( \frac{2L}{\delta} \right)^{9/4} - \left( \frac{\delta}{2L} \right)^{3/4} \right], \quad \delta < 2L \quad (3.5.5)$$

- ◆ The first term in Eq. (3.5.5) arises from the osmotic repulsion between the coils which favors their stretching, and the second term is due to the elastic energy of the chains which opposes stretching.

**Example 3.5.2:** The surface of a material is covered with a water-soluble nonionic polymeric surfactant such that the surface concentration of the surfactant is  $1 \times 10^{-6}$  mol/m<sup>2</sup>. Calculate the repulsive pressure at 298 K when two such surfaces are brought close to each other such that  $\frac{\delta}{2L} = 0.9$ .

**Solution:** Here,  $\Gamma = 1 \times 10^{-6} \times 6.023 \times 10^{23} = 6.023 \times 10^{17}$  m<sup>-2</sup>. The mean distance between the attachment points is,

$$\bar{s} = \left( \frac{1}{\Gamma} \right)^{1/2} = \left( \frac{1}{6.023 \times 10^{17}} \right)^{1/2} = 1.29 \times 10^{-9} \text{ m}$$

Therefore, from Eq. (3.5.5) we get,

$$\Pi_s = \frac{kT}{\bar{s}^3} \left[ \left( \frac{2L}{\delta} \right)^{9/4} - \left( \frac{\delta}{2L} \right)^{3/4} \right] = \frac{1.381 \times 10^{-23} \times 298}{(1.29 \times 10^{-9})^3} \left[ \left( \frac{1}{0.9} \right)^{9/4} - (0.9)^{3/4} \right] = 6.6 \times 10^5 \text{ Pa}$$

## Exercise

**Exercise 3.5.1:** A polymeric surfactant adsorbs at water–oil interface such that its interfacial concentration is  $1 \times 10^{-6}$  mol/m<sup>2</sup> at 298 K. Calculate the steric repulsive force between two parallel ring-surfaces of equal size having 1 mm radius and 50 nm width, if the distance between them is 80% of the total thickness of the brushes on the two ring surfaces.

**Exercise 3.5.2:** Draw the net interaction energy profiles at 298 K for two flat surfaces as per the DLVO theory using the following parameters.

- (i)  $A_H = 2 \times 10^{-20}$  J,  $\psi_0 = 125$  mV and  $c^\infty = 50$  mol/m<sup>3</sup>
- (ii)  $A_H = 3.5 \times 10^{-20}$  J,  $\psi_0 = 35$  mV and  $c^\infty = 100$  mol/m<sup>3</sup>

**Exercise 3.5.3:** Generate the DLVO force-versus-separation profiles shown in Fig. 3.5.5 after going through the article by Pashley and Israelachvili (1984).

**Exercise 3.5.4:** Answer the following questions clearly.

- (a) Discuss the salient features of the DLVO theory.
- (b) Write the names of the four scientists whose names feature in the DLVO theory.
- (c) Explain the effects of (i) Hamaker constant, (ii) surface potential, and (iii) concentration of electrolyte on the profiles of net interaction energy according to the DLVO theory.
- (d) What is critical coagulation concentration?
- (e) What are non-DLVO forces? Why are they called so? Give two examples.
- (f) Explain how polymers stabilize colloid particles. What is bridging?
- (g) Write the de Gennes equation for polymeric steric force and explain the significance of the terms involved in it.

## Suggested reading

### Textbooks

- ◆ P. C. Hiemenz and R. Rajagopalan, *Principles of Colloid and Surface Chemistry*, Marcel Dekker, New York, 1997, Chapter 13.
- ◆ P. Ghosh, *Colloid and Interface Science*, PHI Learning, New Delhi, 2009, Chapter 5.
- ◆ R. J. Hunter, *Foundations of Colloid Science*, Oxford University Press, New York, 2005, Chapter 12.

### Reference books

- ◆ E. J. W. Verwey and J. Th. G. Overbeek, *Theory of the Stability of Lyophobic Colloids*, Dover, New York, 1999, Part II.
- ◆ J. N. Israelachvili, *Intermolecular and Surface Forces*, Academic Press, London, 1997, Chapters 12–14.

### Journal articles

- ◆ J. Israelachvili and H. Wennerström, *Nature*, **379**, 219 (1996).
- ◆ J. Israelachvili and R. M. Pashley, *J. Colloid Interface Sci.*, **98**, 500 (1984).
- ◆ J. S. Clunie, J. F. Goodman and P. C. Symons, *Nature*, **216**, 1203 (1967).
- ◆ P. Claesson, R. G. Horn, and R. M. Pashley, *J. Colloid Interface Sci.*, **100**, 250 (1984).
- ◆ P. G. de Gennes, *Adv. Colloid Interface Sci.*, **27**, 189 (1987).
- ◆ R. M. Pashley and J. Israelachvili, *J. Colloid Interface Sci.*, **97**, 446 (1984).
- ◆ R. M. Pashley, *Adv. Colloid Interface Sci.*, **16**, 57 (1982).
- ◆ R. M. Pashley, *J. Colloid Interface Sci.*, **83**, 531 (1981).